UMYU Scientifica, Vol. 4 NO. 2, June 2025, Pp 309 – 312
https://doi.org/10.56919/usci.2542.030
ISSN: 2955 – 1145 (print); 2955 – 1153 (online)
A periodical of the Faculty of Natural and Applied Sciences, UMYU, Katsina

ORIGINAL RESEARCH ARTICLE

Photocatalytic Properties of ZrS3: A First-Principles Study

Mahmud Abdulsalam[1]
[1]Department of Physics, Umaru Musa Yar'adua University, Katsina State, Nigeria

ARTICLE HISTORY
Received March 27, 2025
Accepted June 28, 2025
Published June 30, 2025

KEYWORDS
band gap photocatalysis DFT

ABSTRACT
The photocatalytic properties of ZrS_3 with $P21/m$ structure were studied using Density Functional Theory (DFT) at the atomic level, vdW-DF and vdW-TS were used to account for the long-range dispersion forces between the layers of the structure, a necessary ingredient for an accurate description of structural properties of any layered structure. The band gap of the structure was calculated at both the DFT and MBJ level of approximation. The MBJ was able to reproduce the reported experimental band gap of about 1.8 eV. Calculated photocatalytic properties of the structure indicated that the structure, in its bulk form, may not be a promising candidate for photocatalysis.

INTRODUCTION

As a result of their potential applications in the field of electronic, nanotechnology, superconductivity, and energy conversion, Transition metal chalcogenides (TMCs) have recently gained the attention of researchers from all areas of science and engineering. The Tran- sition Metal Chalcogenides (TMC) are family of com- pounds with general formula M_yQ_z, where M belongs to the family of transition metals (V, Nb, Ta, Cr, Mo, W, Mn, Tc or Re), and Q represents the chalcogen family (P, S, Se and Te), y and z are integers. They have a variety of potentially useful properties (Benameur et al., 2011; Kumar & Ahluwalia, 2012; Radisavljevic et al., 2011; Mak et al., 2013; Yin et al., 2011). These materials possess a layered structure and exhibit unique properties because of the interplay between electron-phonon and electron-electron interactions (He et al., 2019). TMCs are promising materials as efficient photocatalysts for carbon IV oxide reduction, hydrogen evolution and oxygen evolution, as a result of their high electrochemical tunability and superior electrical conductivity (Nath et al., 2022). Recently, researchers have focused on possible ways to optimise TMCs for photocatalysis, addressing challenges in electrocatalytic or photocatalytic activity and long-term stability (Liu et al., 2023). In short, TMCs present a promising avenue for advancing sustainable energy technologies and novel electronic applications.

It is surprising that within the TMCs, there is little or no information on the photocatalytic properties of ZrS_3. This lack of information appears surprising considering its reported favourable band gap (Abdulsalam & Joubert, 2015; Perluzzo et al., 1980). ZrS_3 crystallises in a monoclinic structure of space group $P21/m$ with $Z = 2$. Its basic structure is composed of prismatic trigonal columns of M_2X^6 (M = Ti, Hf or Zr and X = S, Se or Te) linked to form layers, which are in turn bonded by a weak van der Walls forces. The metal Zr is at the centre of the prism, connected to six sulphide atoms at the corners and to two other sulphide atoms in the neighbouring chains. The bandgap of the class M_2X_6 (M = Ti, Hf or Zr and X = S, Se or Te) has been reported by several authors (Abdulsalam & Joubert, 2015; Ait-Ouali & Jandl, 1996). The band gap is an essential ingredient for the calculation of the photocatalytic properties of the ZrS_3. The photocatalysis involves the production of hydrogen from water using solar energy for the supply of recyclable and clean energy (Fujishima & Honda, 1972; Grätzel, 2001). The process of water splitting involves the oxidizing and reducing ability of the semiconductor photocatalyst. A photocatalyst is required to have its conduction band minimum (CBM) more negative than the reduction potential of hydrogen, its valence band maximum more positive than the oxidation potential of water and a band gap of about 2 eV to be able to split the water without the aid of external electric power (Osterloh & Parkinson, 2011; Walter et al., 2010).

The calculations in this paper were done using density functional theory (KS-DFT) with the inclusion of van der Waals forces to study the structural and electronic properties of ZrS_3 as input for the computation of the photocatalytic properties of the structure. It is established that KS-DFT is lacking in accurately describing the electronic properties of semiconductors and is sometimes underestimated by as

Correspondence: Mahmud Abdulsalam. Department of Physics, Umaru Musa Yar'adua University, Katsina State, Nigeria.
✉ afdalmah@gmail.com
How to cite: Abdulsalam, M. (2025). Photocatalytic Properties of ZrS3: A First-Principles Study. *UMYU Scientifica*, 4(2), 309 – 312. https://doi.org/10.56919/usci.2542.030

much as 30 per cent (Aryasetiawan & Gunnarsson, 1998). Interestingly, Post-DFT methods required for improving the accuracy of the DFT band gaps, such as many-body perturbation techniques (GW and BSE methods), are computationally very expensive. In trying to overcome this, we employ the application of Modified Becke-Johnson potential (MBJ) (Tran & Blaha, 2009), a method which is not as computationally demanding as the GW methods, but known to yield electronic properties at an accuracy comparable to the hybrid and GW methods, to estimate the band gaps. In order to have a better picture of the electronic properties of the structure, the MBJ calculations were carried out with and without the inclusion of perturbative spin orbit coupling.

COMPUTATIONAL METHODOLOGY

In this paper, we used Kohn-Sham Density Functional Theory (Kohn & Sham, 1965; Hohenberg & Kohn, 1964) coupled with a van der Waals correction term proposed by Tkatchenko & Scheffler (2009) and Dion et al. (2004) are first used to study the structural and electronic properties of ZrS_3 in $P\,21/m(11)$ structure. The projector augmented wave (PAW) (Kresse & Joubert, 1999) scheme as implemented in the Vienna ab initio Simulation Package (VASP) (Kresse & Hafner, 1994; Kresse & Hafner, 1993) is used to mimic electron- ion interaction, while the Perdew, Burke and Ernzerhof (PBE) (Ernzerhof & Scuseria, 1999; Perdew, Burke, & Ernzerhof, 1996) parametrization of the generalised gradient approximation (GGA) (Becke, 1988; Perdew et al., 1992; Perdew et al., 1993) is used for exchange correlation in the vdW-TS implementation. 8 × 6 × 4 Monkhorst-Pack meshes for sampling the Brillouin zones with an energy cut-off of 520 eV were sufficient for energy convergence. The Brillouin zone sampling was chosen in such away that the convergence of free energy is less than 1 MeV/atom.

Table 1: Calculated and experimental equilibrium parameters of ZrS_3: lattice constants [a (Å), b (Å), c (Å)], volume V_0 (Å³), formation energy E_f per atom and cohesive energy E_{coh} per atom.

Function	a (Å)	b (Å)	C (Å)	V_0 (Å³)	E_f (eV/atom)	E_{coh} (eV/atom)	β°
vdW-TS	5.04	3.63	9.05	164.74	-1.15	-5.36	96.95
vdW-DF	5.21	3.66	9.15	174.04	-1.37	-5.21	96.05
Experiment	5.12 [a]	3.62 [a]	8.98	164.40 [a]			97.28 [a]

a = reference: Brattas & Kjekshus (1972)

RESULTS AND DISCUSSION

Structural properties

Accurate description of the photocatalytic properties relies upon an accurate description of the electronic properties of any structure, which in turn depends upon an accurate description of the structural properties of such a structure. We therefore begin our calculations with structural optimisation for the ZrS_3 structure. The structure was distorted, allowing the atoms to move, and we calculated the cohesive and formation energy at each atomic site. The point with the least cohesive and formation energy is considered as the point where the structure is most stable, and all subsequent computations are done at that point, but first taking note of the structural parameters at that point. The computed structural parameters for the two approximations used are depicted in Table 1, and our computed values are compared with the experimental reported values. From the table, it is evident that both the vdW-TS and vdW-DF slightly overestimate the reported experimental value of the interlayer distance c by at least 0.07 of its original value. This is an indication of the dispersion correction terms to accurately account for the interlayer distance in the ZrS_3-like structures. We also note that the vdW-TS predicts other structural parameters and volume of this structure that are in better agreement with the reported experimental value. We therefore decided to use the vdW-TS reported values for our MBJ calculations for better accuracy.

Table 2. Calculated and experimental energy band gaps (in eV) of ZrX_3 (X = S, Se, Te).

Compound	vdW-TS	vdW-DF	MBJ	Experimental
ZrS_3	1.02	1.20	1.80	2.00 [c], 2.01 [b,c]
$ZrSe_3$	–	–	–	–
$ZrTe_3$	–	–	–	–

b = reference: Kurita et al. (1993), c = reference: Adachi et al. (1980)

Electronic properties

The band structure and spin projected density of states (DOS) of ZrS_3 are plotted in Figure 1. Spin projected total density of states (TDOS) is shown in sub-figures (b). Since the structure is non-magnetic, electrons occupy the spin-up and spin-down bands equally, leading to a zero spin-polarised density of states; we showed only one component of the spin contribution.

ZrS_3 is an indirect band gap semiconductor. Its conduction band minimum is at Y, and its valence band maximum is at a point between Γ and Z of the high symmetry points.

Photocatalytic properties

To study the photocatalytic properties of ZrS_3, we need to calculate the valence band (VB) and conduction band (CB) edges of ZrS_3 based on the DFT slab calculations and Mulliken's absolute electronegativity (Mulliken, 1934; Nethercot, 1974). Here, the ionisation potential can be calculated from the difference between the electrostatic potential in a vacuum V_{vac}^{S} and the energy of the valence band maximum ϑ_{VBM}^{S} given by $I^{KS} = V_{vac}^{S} - \varepsilon_{VBM}^{S}$ (Jiang & Shen, 2013) and the electron affinity by $A \equiv I^{KS} - E_G$ where E_g is the DFT band gap of the ZrS_3 structure. The absolute electronegativity is calculated in the Mul- likan's terms is defined as the average of the electron affinity and the ionisation potential of the ZrS_3, $\chi = \frac{1}{2}(I + A)$ and it is the tendency to attract or denote an electron by the atom. The absolute electronegativity of a structure, say, M_pX_n, is also defined in this model from the mean geometric electronegativities of the constituent atoms using the formulae (Xu & Schoonen, 2000) $E_{VB} = \chi(M)^p\chi(X)^{n\frac{1}{p+n}} - E_e + 0.5E_g$ and $E_{CB} = E_{VB} - E_g$. The E_{CB} and E_{VB} here are the CB and the VB edges. E_g is the calculated band gap, and E_e is the standard electrode potential on the hydrogen scale, which is about 4.5 eV. From the Pearson table, the absolute electronegativity of $\chi_S = 6.22$ and that of $\chi_{Zr} = 3.64$, using which, we can calculate the E_{CB} and E_{VB} of the ZrS_3. For ZrS_3, we found the electronegativity to be 3.44 eV, which gives us E_{VB} of −0.16 and E_{CB} of −1.96. This result indicates that ZrS_3 has its VB edge at −0.16, which is lower than that of water (O2/H2O, 1.23 V), and CB edge potential at −1.96. Therefore, ZrS_3 in its bulk form may not be a good material for photocatalytic applications.

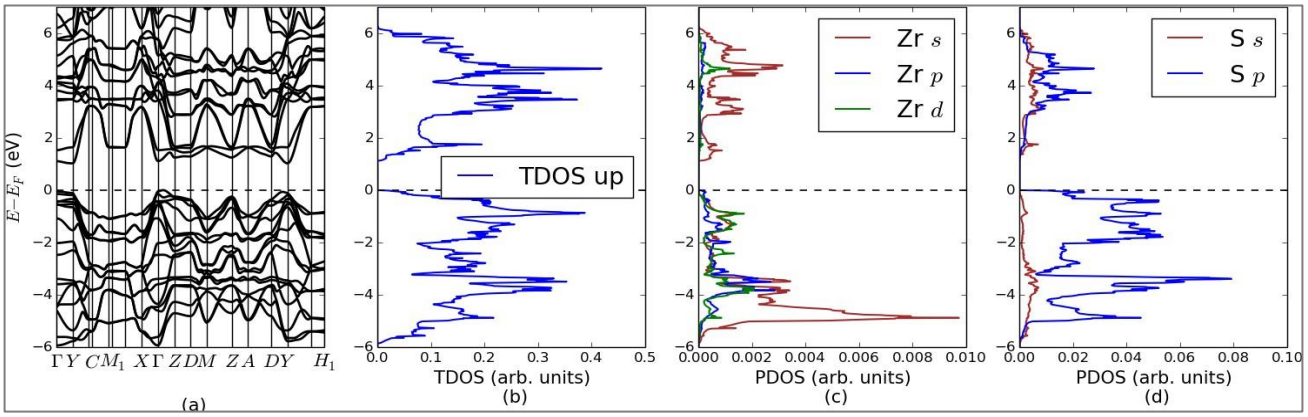

Figure 1: ZrS3 vdW-TS ca cu ated band structure (a) band structure a ong h gh symmetry K-po nts, (b) sp n projected tota dens ty of states (TDOS), (c) part dens ty of states (PDOS) of Zr(s,p,d) (d) PDOS of S (s,p).

REFERENCES

Abdulsalam, M., & Joubert, D. P. (2015). Structural and electronic properties of MX_3 (M = Ti, Zr and Hf; X = S, Se, Te) from first principles calculations. *The European Physical Journal B, 88*, 1–11. [Crossref]

Adachi, T., Goto, T., & Nishina, Y. (1980). Photoluminescence from excitons in ZrS_3. *Journal of Luminescence, 21*(2), 169–175. [Crossref]

Ait-Ouali, A., & Jandl, S. (1996). Photoluminescence study of the one-dimensional material ZrS_3 and its solid solution $Zr_{1-x}Hf_xS_3$. *Physical Review B, 53*(15), 9852. [Crossref]

Aryasetiawan, F., & Gunnarsson, O. (1998). The GW method. *Reports on Progress in Physics, 61*(3), 237. [Crossref]

Becke, A. D. (1988). Density-functional exchange-energy approximation with correct asymptotic behavior. *Physical Review A, 38*(6), 3098. [Crossref]

Benameur, M., Radisavljevic, B., Heron, J., Sahoo, S., Berger, H., & Kis, A. (2011). Visibility of dichalcogenide nanolayers. *Nanotechnology, 22*(12), 125706. [Crossref]

Brattas, L., & Kjekshus, A. (1972). Properties of compounds with $ZrSe_3$-type structure. *Acta Chemica Scandinavica, 26*(9), 3441–3449. [Crossref]

Dion, M., Rydberg, H., Schröder, E., Langreth, D. C., & Lundqvist, B. I. (2004). Van der Waals density functional for general geometries. *Physical Review Letters, 92*(24), 246401. [Crossref]

Ernzerhof, M., & Scuseria, G. E. (1999). Assessment of the Perdew-Burke-Ernzerhof exchange-correlation functional. *The Journal of Chemical Physics, 110*(11), 5029–5036. [Crossref]

Fujishima, A., & Honda, K. (1972). Electrochemical photolysis of water at a semiconductor electrode. *Nature, 238*(5358), 37–38. [Crossref]

Grätzel, M. (2001). Photoelectrochemical cells. *Nature, 414*(6861), 338–344. [Crossref]

He, Y., Yan, D., Shi, L., Wang, S., Xie, Z., & Luo, H. (2019). Review of nanoscale layered transition metal chalcogenide superconductors. *Advanced Materials Letters, 10*(3), 152–163. [Crossref]

Hohenberg, P., & Kohn, W. (1964). Density functional theory (DFT). *Physical Review, 136*, B864. [Crossref]

Jiang, H., & Shen, Y.-C. (2013). Ionization potentials of semiconductors from first-principles. *The Journal of Chemical Physics, 139*(16). [Crossref]

Kohn, W., & Sham, L. J. (1965). Self-consistent equations including exchange and correlation effects. *Physical Review, 140*(4A), A1133. [Crossref]

Kresse, G., & Hafner, J. (1993). *Ab initio* molecular dynamics for liquid metals. *Physical Review B, 47*(1), 558. [Crossref]

Kresse, G., & Hafner, J. (1994). *Ab initio* molecular-dynamics simulation of the liquid-metal-amorphous-semiconductor transition in germanium. *Physical Review B, 49*(20), 14251. [Crossref]

Kresse, G., & Joubert, D. (1999). From ultrasoft pseudopotentials to the projector augmented-wave method. *Physical Review B, 59*(3), 1758. [Crossref]

Kumar, A., & Ahluwalia, P. (2012). Electronic structure of transition metal dichalcogenides monolayers 1H-MX_2 (M = Mo, W; X = S, Se, Te) from ab-initio theory: New direct band gap semiconductors. *The European Physical Journal B - Condensed Matter and Complex Systems, 85*(6), 1–7. [Crossref]

Kurita, S., Tanaka, M., & Levy, F. (1993). Optical spectra near the band edge of ZrS_3 and $ZrSe_3$. *Physical Review B, 48*(3), 1356. [Crossref]

Liu, Y., Guo, Y., Liu, Y., Wei, Z., Wang, K., & Shi, Z. (2023). A mini review on transition metal chalcogenides for electrocatalytic water splitting: Bridging material design and practical application. *Energy & Fuels, 37*(4), 2608–2630. [Crossref]

Mak, K. F., He, K., Lee, C., Lee, G. H., Hone, J., Heinz, T. F., & Shan, J. (2013). Tightly bound trions in monolayer MoS_2. *Nature Materials, 12*(3), 207–211. [Crossref]

Mulliken, R. S. (1934). A new electroaffinity scale; together with data on valence states and on valence ionization potentials and electron affinities. *The Journal of Chemical Physics, 2*(11), 782–793. [Crossref]

Nath, M., Singh, H., & Saxena, A. (2022). Progress of transition metal chalcogenides as efficient electrocatalysts for energy conversion. *Current Opinion in Electrochemistry, 34*, 100993. [Crossref]

Nethercot, A. H., Jr. (1974). Prediction of Fermi energies and photoemission thresholds based on electronegativity concepts. *Physical Review Letters, 33*(18), 1088. [Crossref]

Osterloh, F. E., & Parkinson, B. A. (2011). Recent developments in solar water-splitting photocatalysis. *MRS Bulletin, 36*(1), 17–22. [Crossref]

Perdew, J. P., Burke, K., & Ernzerhof, M. (1996). Generalized gradient approximation made simple. *Physical Review Letters, 77*(18), 3865. [Crossref]

Perdew, J. P., Chevary, J. A., Vosko, S. H., Jackson, K. A., Pederson, M. R., Singh, D. J., & Fiolhais, C. (1992). Atoms, molecules, solids, and surfaces: Applications of the generalized gradient approximation for exchange and correlation. *Physical Review B, 46*(11), 6671. [Crossref]

Perdew, J. P., Chevary, J., Vosko, S., Jackson, K. A., Pederson, M. R., Singh, D., & Fiolhais, C. (1993). Erratum: Atoms, molecules, solids, and surfaces: Applications of the generalized gradient approximation for exchange and correlation. *Physical Review B, 48*(7), 4978. [Crossref]

Perluzzo, G., Jandl, S., & Girard, P. (1980). Optical spectra of ZrS_3. *Canadian Journal of Physics, 58*(1), 143–145. [Crossref]

Radisavljevic, B., Radenovic, A., Brivio, J., Giacometti, V., & Kis, A. (2011). Single-layer MoS_2 transistors. *Nature Nanotechnology, 6*(3), 147–150. [Crossref]

Tkatchenko, A., & Scheffler, M. (2009). Accurate molecular van der Waals interactions from ground-state electron density and free-atom reference data. *Physical Review Letters, 102*(7), 073005. [Crossref]

Tran, F., & Blaha, P. (2009). Accurate band gaps of semiconductors and insulators with a semilocal exchange-correlation potential. *Physical Review Letters, 102*(22), 226401. [Crossref]

Walter, M. G., Warren, E. L., McKone, J. R., Boettcher, S. W., Mi, Q., Santori, E. A., & Lewis, N. S. (2010). Solar water splitting cells. *Chemical Reviews, 110*(11), 6446–6473. [Crossref]

Xu, Y., & Schoonen, M. A. (2000). The absolute energy positions of conduction and valence bands of selected semiconducting minerals. *American Mineralogist, 85*(3–4), 543–556. [Crossref]

Yin, Z., Li, H., Li, H., Jiang, L., Shi, Y., Sun, Y., Lu, G., Zhang, Q., Chen, X., & Zhang, H. (2011). Single-layer MoS_2 phototransistors. *ACS Nano, 6*(1), 74–80. [Crossref]